Contents lists available at ScienceDirect

Journal of the Mechanics and Physics of Solids

journal homepage: www.elsevier.com/locate/jmps

ViscoNet: A lightweight FEA surrogate model for polymer nanocomposites viscoelastic response prediction

Anqi Lin, Richard J. Sheridan, Bingyin Hu, L. Catherine Brinson *

Department of Mechanical Engineering and Materials Science, Duke University, Durham, NC 27708, USA

ARTICLE INFO

Keywords:
Material design
Polymer nanocomposites
Surrogate model
Viscoelasticity

ABSTRACT

Polymer-based nanocomposites (PNCs) are formed by dispersing nanoparticles (NPs) within a polymer matrix, which creates polymer interphase regions that drive property enhancement. However, data-driven PNC design is challenging due to limited data. To address the challenge, we present ViscoNet, a surrogate model for finite element analysis (FEA) simulations of PNC viscoelastic (VE) response. ViscoNet leverages pre-training and finetuning to accelerate predicting VE response of a new PNC system. By predicting the entire VE response, ViscoNet surpasses previous scalar-based surrogate models for FEA simulation, offering better fidelity and efficiency. We explore ViscoNet's effectiveness through generalization tasks, both within thermoplastics and from thermoplastics to thermosets, reporting a mean absolute percentage error (MAPE) of < 5 % for rubbery modulus and < 1 % for glassy modulus in all cases and 1.22 % on tan δ peak height prediction. With only 500 FEA simulations for finetuning, ViscoNet can generate over 20k VE responses within 2 min with 1 CPU, compared to 97 days with 4 CPUs via FEA simulations.

1. Introduction

Polymer-based nanocomposites (PNCs) are materials that combine polymers with nanoscale fillers, forming a material that has enhanced properties. These nanofillers can be NPs of various materials such as metals (Faupel et al., 2010), metal oxides (Khan et al., 2015), clays (Li et al., 2003), carbon-based materials like nanotubes (Wang et al., 2005) or graphene (Pham et al., 2012), and more. The geometric and chemical interactions between polymer chains and NPs at the interface creates a region known as the "interphase" which causes the property enhancement seen in polymer nanocomposites (Liu et al., 2016). Studies have shown that properties of some interphases can be approximated by modifying the pure polymer matrix properties by frequency shifting or broadening around the tan δ peak (Li et al., 2019), (Wang et al., 2018).

Materials design continues to be a time-consuming process that spans several years to decades, requiring a deep understanding of the complex relationships between processing, structure, and properties (p-s-p relationships) of materials (Schadler et al., 2020), (W. Chen et al., 2020). Viscoelastic properties play a crucial role in determining the performance of PNCs, and thus both understanding and accurately predicting viscoelastic properties are essential. In recent years, data-driven prediction methods have gained popularity due to their ability to learn intricate relationships and have shown promise in aiding understanding p-s-p relationships, provided there is sufficient data available (Deagen et al., 2022), (Himanen et al., 2019), (Xu et al., 2021), which is often not the case for PNCs. To address this data limitation, our growing FAIR data resource, MaterialsMine, has emerged to make data more accessible and comprehensive

* Corresponding author.
E-mail address: cate.brinson@duke.edu (L.C. Brinson).

https://doi.org/10.1016/j.jmps.2024.105915
Received 5 April 2024; Received in revised form 26 August 2024; Accepted 17 October 2024

(Zhao et al., 2016), (Zhao et al., 2018), (Brinson et al., 2020), (Prabhune et al., 2023).

While efforts are being made to increase the availability of experimental PNC data, the finite element analysis (FEA) simulations can presently generate a significant amount of data in a shorter time span. In the computational materials community, high-throughput density functional theory (DFT) simulations have proven successful in rapidly exploring a wide range of candidate materials for subsequent experimental investigation (Gossett et al., 2018), (Mehl et al., 2017). Similarly, FEA simulations can be applied to exploration of the PNC design space. However, FEA simulations are computationally expensive and time-consuming. Therefore, there is a need to create a surrogate model that is computationally efficient (Hashemi et al., 2023), and can ideally be effectively used on a personal laptop in low-resource settings. The development of inexpensive surrogate models helps democratize material design by enabling resource-constrained engineers, companies, and countries to actively participate in the exploration and optimization of PNCs.

Surrogate models are widely adopted in the materials science community for constitutive modeling (Liu et al., 2021). Since the emergence of the Artificial Neural Network (ANN), with its powerful capability of modeling non-linearity, it has been widely applied as a surrogate model, with some early adopters considered its application on PNCs nearly two decades ago (Zhang and Friedrich, 2003). Zhang et al. made an early attempt using a 1-layer feed forward neural network with a hidden size of 25 on 480 experimental data for storage modulus and tan δ prediction at given temperature (Zhang et al., 2002). Over the years, a variety of ANN models were introduced and applied by researchers on materials science modeling. Recurrent Neural Network (RNN) is a special type of ANN that recurrently uses the hidden state emitted by the neuron as input to the next state, granting it the capability of sequential predictions (Rumelhart et al., 1986), (Hochreiter and Schmidhuber, 1997). Wu et al. utilized a Gated Recurrent Unit (GRU)-based RNN as a surrogate model for micro-scale simulations within the framework of multi-scale analysis in solid mechanics (Wu et al., 2020). The use of RNN enables the model to predict the stress history. Similarly, Chen et al. utilized the Long-Short Term Memory (LSTM) model, another type of RNN model, as a surrogate for finite-volume direct averaging micromechanics modeling of elastoplastic response of heterogeneous materials (Chen et al., 2021). Convolutional Neural Network (CNN) is widely used in image/topology-related tasks due to its convolutional and pooling layers for feature extraction from images (LeCun et al., 1998).

Nie, et al. demonstrated that CNN can be used for stress field prediction in a homogenous cantilever (Nie et al., 2020). Chen et al. trained a CNN model as an FEA surrogate for thermo-mechanical properties simulation of unidirectional composites (Q. Chen et al., 2020). FEA-Net incorporates knowledge in physics into the CNN for mechanical response prediction with better physical interpretation and supports multi-phrase systems like PNCs (Yao et al., 2020). Another recent work utilized microstructure images of PNCs as input to CNN for viscoelastic properties prediction, including tan δ peak, glassy modulus, and rubbery modulus (Wang et al., 2020).

Despite the progress made, there are several challenges in ANN surrogate modeling of PNCs that need to be addressed. First, existing surrogate models for PNC FEA simulations often have restricted parameter spaces and are specific to materials systems or other parameters. Second, these models often predict scalar metrics derived from the viscoelastic (VE) response curve, rather than the full curve itself. Lastly, many surrogate models like RNN and CNN are themselves computationally slow and require extensive resources.

To overcome these challenges, we propose a novel surrogate model, ViscoNet, for FEA simulations of PNC VE response prediction. ViscoNet leverages the pre-training then finetuning training scheme, inspired by successful approaches used in the natural language processing (NLP) domain (Devlin et al., 2019), (Raffel et al., 2020), (OpenAI 2023). Pre-training the model with a large dataset covering a wide parameter space enables it to capture general understanding of VE response. Subsequently, the model is finetuned with a smaller dataset specific to the materials system of interest, refining its knowledge for accurate predictions. We utilize a simple multilayer perceptron (MLP) architecture, offering fast training and inference times. To address the issue of reducing the VE response to an ANN input vector, we employ a frequency-fixing technique, transforming the 2D spectral response curve into a 1D series. In this work, we present our surrogate model for PNC VE response prediction, which demonstrates good fidelity and efficiency.

2. Material and methods

2.1. Design space

2.1.1. Microstructure generation

15 random seeds were used to generate 15 sets of microstructures using the combination of parameters described in Table 1.

All microstructures were generated as a 500px-by-500px square grid, representing a physical size of 1μm-by-1μm. Note that the standard deviation of particle radius is limited to 20 %−60 % of the mean particle radius. For example, if the mean radius is 20 nm, then possible parameter combinations are 20 ± 5 nm and 20 ± 10 nm because the standard deviation is bounded by 4 nm and 12 nm. Particles are positioned randomly without overlap and sequentially until the desired volume fraction is reached; no particle agglomeration is considered in this work. For a given particle distribution, we only increase the interphase thickness until it saturates

Table 1
Parameter space for microstructure generation.

Parameters	Parameter space
Particle radius mean	[5, 10, 20, 35, 50] [nm]
Particle radius std. deviation	[1, 3, 5, 10, 20, 30] [nm] bounded by [0.2 mean, 0.6 mean]
Fixed RVE size	500 [pixel]
Particle volume fraction	[0.05, 0.10, 0.15, 0.20, 0.25, 0.30, 0.35, 0.40, 0.45, 0.50]
Interphase thickness	[0, 10, 20, 30, 40, 50, 60, 70, 80, 90, 100] [nm]

as a two-phase, particle-interphase-only material. Thus, for certain cases, the interphase thickness might be capped at a value smaller than 100 nm since higher thicknesses would result in identical material systems with identical performance. Overall, in this design of experiments (DOE) from Table 1, 11,289 microstructures were generated.

2.1.2. FEA simulation

2D FEA simulations for VE response of PNCs were done with Abaqus. The pixel-based image was converted into a 500-by-500 mesh with four-node plane strain element CPE4R. A 0.5 % tension displacement in x direction was applied to a reference node kinematically coupled to boundary nodes. Periodic boundary conditions as implemented in (Li et al., 2019) and (Qiao and Catherine Brinson, 2009) were assumed. For the output VE response, 30 intervals were evenly distributed on a log scale between 10^{-4} Hz and 10^{3} Hz.

To model the interphase properties, we include a shifting factor in {−3, −2, −1}, which indicates shifting the matrix viscoelastic properties towards lower frequency by 1 to 3 decades, and a broadening factor in {1, 2, 3}, with 1 being no broadening and 3 being widening the frequency range anchored at the tan δ peak by 3 times (Wang et al., 2018). These conditions are most appropriate for attractive interactions between the particle surface and matrix.

2.1.3. Materials system

Studies have shown that the viscoelastic properties of PNC are minimally impacted by the NP modulus, both in terms of the magnitude and the isotropy (Qiao and Catherine Brinson, 2009). For nanofiller, we picked isotropic elastic silica NPs with a density of 2.65 g/cm^3, a Young's modulus of 73 GPa, and a Poisson's ratio of 0.17. For the polymer matrix, Table 2 summarizes the thermoplastics and thermosets that we examined for the generalization experiments. For thermoplastics, we examined polycarbonate (PC), polymethyl methacrylate (PMMA), and polystyrene (PS). For thermosets, we picked an epoxy.

2.2. Feature engineering

ViscoNet uses two groups of input features: spectral and scalar. As mentioned earlier, we flattened the 2D VE spectral data into a feature vector by evaluating the response at fixed frequency output by Abaqus, resulting in 30 features.

For VE response, there are three curves of interest, namely storage modulus (E'), loss modulus (E''), and tan δ. At a given frequency, the relation between these quantities is defined by $tan\ \delta\ = E''/E'$. Thus, one can predict just two of these three properties and trivially calculate the third. In this work, ViscoNet seeks to predict tan δ curves and E' curves, since an E'' curve can be generated from those without performing division with a predicted value that may contain substantial error, i.e., generating a Cauchy-distributed prediction.

There are two extra processing steps for the spectral features. Since E' can range from MPa to GPa, instead of predicting the E', VisoNet predicts the base 10 logarithm log(E') for numerical stability. To make sure that ViscoNet can handle all types of input and for faster convergence, the magnitude of the input log(E') curves and tan δ curves are each scaled by

$$X_{i,\ scaled} = \frac{X_i - min(X)}{max(X) - min(X)}$$

$$Y_{i,\ scaled} = \frac{Y_i - min(X)}{max(X) - min(X)}$$

where X stands for the 30 input log(E') or tan δ values of pure polymer matrix at fixed frequency, and Y stands for the corresponding values of PNCs at those frequency. Note that Y is also scaled with the min and max of X. During inference, the (unscaled) VE spectral data of pure polymer matrix is provided as original input, so we can use the scaling values to obtain the actual (non-scaled) values of the predicted composite property curves. Fig. 1 demonstrates the VE response curves of polymer matrices before and after scaling.

In addition to the spectral data features, ViscoNet also uses an array of scalar features, including mean and standard deviation of particle radius (ParRu and ParRv), volume fraction of free particles (Vf), volume fraction of interphase (Vt), shifting factor, broadening factor, and a binary percolation flag as input. Percolation happens when the interphase overlaps and forms a pathway across the PNC, as illustrated in Fig. 2. Percolation is determined by a Depth-First Search from left to right and top to bottom. It has been shown that percolation can bring different levels of property change to the PNC, contingent on the strength of interaction between the polymer matrix and NPs (Qiao and Catherine Brinson, 2009), (Zare and Rhee, 2018), (Song and Zheng, 2015).

2.3. ViscoNet

To create our surrogate model, ViscoNet, we evaluated an array of Neural Network (NN) models with two hidden layers, including a

Table 2
Properties of polymer matrices used in this study and the FEA data size generated for the associated polymer-silica nanocomposites.

Polymer	Type	Long-term modulus (MPa)	Density (g/cm^3)	Data size
PC (Fisher et al., 2004)	thermoplastic	3.04	1.2	41,209
PMMA (Alves et al., 2004)	thermoplastic	7.11	1.2	41,389
PS (Cavaille et al., 1987)	thermoplastic	0.001	1.05	47,165
Epoxy (Woo et al., 1991)	thermoset	136.7	1.265	23,005

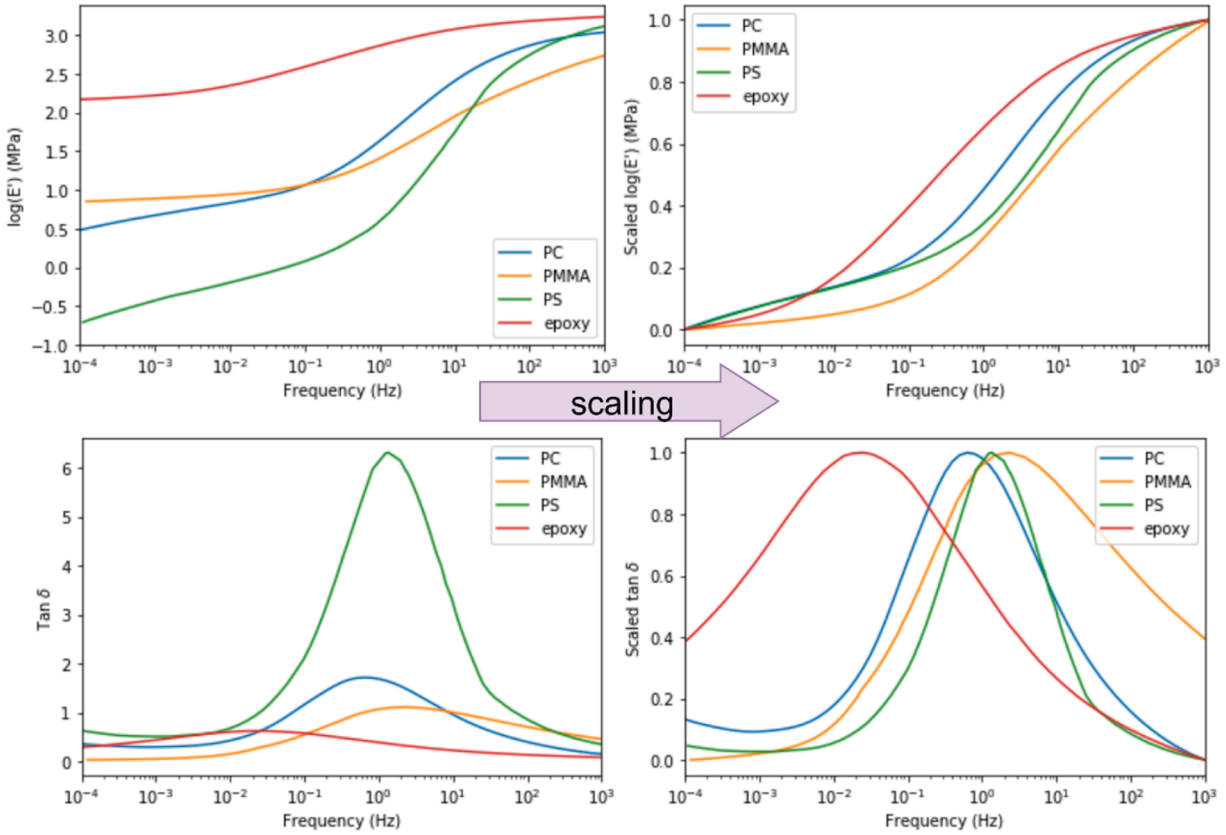

Fig. 1. Log(E') (top) and tan δ (bottom) curves of PC, PMMA, PS, and epoxy, before (left) and after (right) scaling.

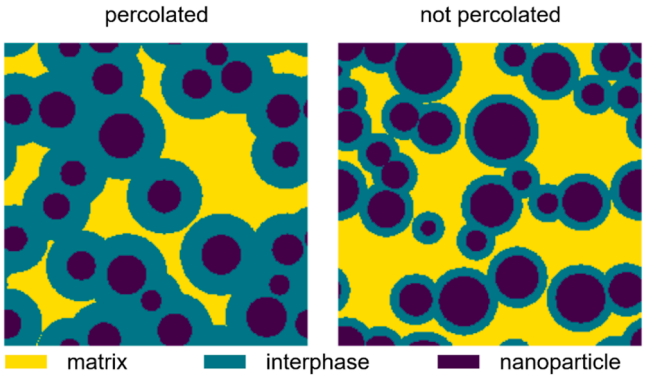

Fig. 2. Illustration of microstructures with (left) and without (right) percolation.

deep NN model with hidden size 128, a deep NN model with hidden size 256, and a Wide-and-Deep NN (WDNN) model with hidden size 256. All NN models have 2 hidden layers. Between every pair of fully connected layers, a Gaussian Error Linear Unit (GELU) activation layer and a dropout of 0.2 are implemented (Hendrycks and Gimpel, 2023). Finetuning and inference with the candidate ViscoNet models, which are lightweight and low resource, do not require GPU. Illustration of these models are shown in Fig. 3.

WDNN is a well-known NN model for recommender systems (Cheng et al., 2016). Its highlight is that it concatenates important categorical features directly to the last hidden layer so that the model memorizes them. Though we do not have categorical features other than the percolation flag in our feature set, we do know that features like shifting and broadening have a big impact on the VE response. Thus, we also evaluated WDNN with different wide feature selections from our scalar features. Table 3 summarizes the model setups evaluated for ViscoNet.

Regardless of network architecture, MSE loss is picked as the training criteria. The NN models were trained on log(E') and tan δ, but not simultaneously which consistently yielded poor performance. Details of training configurations are available in the Supplementary

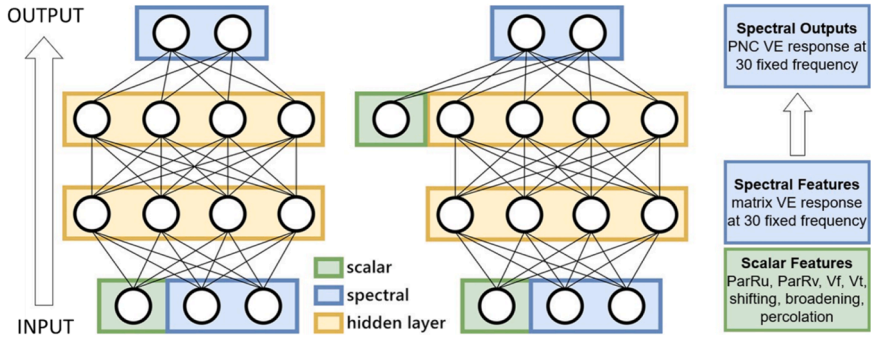

Fig. 3. Deep NN (left) and Wide-and-Deep NN (right) evaluated for ViscoNet.

Table 3
Specifications of NN models evaluated for ViscoNet.

Model code	Hidden size	Has percolation?	Wide feature
VE128np	128	No	N/A
VE128	128	Yes	N/A
VE256	256	Yes	N/A
VE256WDNN5	256	Yes	ParRu, ParRv, shifting, broadening, percolation
VE256WDNN3	256	Yes	shifting, broadening, percolation

Information section S1. The train/valid/test split is by default 64/16/20, unless otherwise specified.

We evaluate the model by the full curve with MSE loss, and by single-point VE properties that can be induced from the predicted VE response curve like peak value for tan δ curves and rubbery/glassy modulus for E' curves with Mean Average Percentage Error (MAPE).

As mentioned earlier, tan δ curve has a complicated bell shape with many possible asymmetries. As you can see from the example in Fig. 4, we can categorize the misprediction of the model into two main types: one for the "shelf" error and the other for peak over- and under-prediction. Our observation from a preliminary study with 10k PS data is that "shelf" error can be reflected by a high full-curve MSE loss, while the peak over/under-prediction error can be reflected by the MAPE of tan δ peak.

3. Results and discussion

In this section, results from our numerical experiments that evaluate ViscoNet's capability of generalization from PC, PMMA (thermoplastics) to PS (thermoplastics) and from PC, PMMA, PS (thermoplastics) to epoxy (thermosets) are reported. Table 4 summarizes the major pre-training and finetuning experiments. Each model architecture listed in Table 3 was pre-trained and finetuned to predict the full PNC VE response curves log(E') and tan δ.

An impact analysis on the percolation feature is presented in Section 3.3, where we compare the number of tan δ predictions with "shelf" error with and without the percolation flag. Another few-shot experiment to discover the progression of model performance with an increasing data size for finetuning is reported in Section 3.4. To quantify the gain of ViscoNet in terms of compute time, estimations are given in Section 3.5. A few use case scenarios are provided and discussed in Section 3.6, along with a few limitations listed in Section 3.7.

3.1. Generalization within thermoplastics

In this subsection, we evaluate the ability of candidate ViscoNet models trained with VE response curves of thermoplastic-based PNC to generalize to a new thermoplastic-based PNC with limited examples for finetuning. ViscoNet was pre-trained with 41,209 PC data points and 41,389 PMMA data points. Then, the pre-trained model was finetuned with only 500 PS data points to predict VE

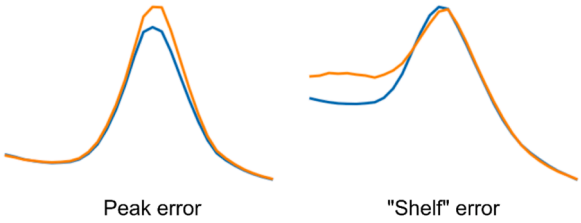

Fig. 4. Peak over/under-prediction error and "shelf" error of tan δ curve.

Table 4
Major pre-training and finetuning experiments conducted in this work.

Experiment Steps	Generalization within thermoplastics		Generalization from thermoplastics to thermosets	
Pre-training data	41,209 PC + 41,389 PMMA		41,209 PC + 41,389 PMMA + 34,964 PS	
Finetuning data	500 PS		500 epoxy	
Test data	23,119 PS		22,505 epoxy	
Output VE response	log(E')	tanδ	log(E')	tanδ

responses of PS-based PNC, without freezing any model parameters. 400 PS data were used for training and the 100 remaining were used for validation. Pre-training required ~30 min for every 50 epochs, resulting in 30 min training time for tan δ models and 60 min for log(E') models. Finetuning on only 1 CPU for 50 epochs takes 15 min with parallel data loading disabled. The finetuned model was evaluated on a test set of 23,119 PS data. All PS data used different microstructures from those used in PC and PMMA FEA simulation.

ViscoNet models of 5 different NN architectures were evaluated by test MSE loss for both log(E') and tan δ prediction, totaling at 10 different NNs. For log(E') prediction, we also report MAPE of rubbery modulus and glassy modulus. For tan δ prediction, we also report MAPE of tan δ peak. Table 5 summarizes the results.

ViscoNet models can predict the glassy modulus with < 0.5 % MAPE and the rubbery modulus with < 6 % MAPE. For log(E') prediction, VE256 achieved the best performance, and the addition of the wide signals seem to hurt the performance, though the decrease is marginal. The result is plausible as E' curves tend to be simpler in shape as compared to tan δ curves, meaning that it might not benefit much from complex structures like WDNN. The percolation signal does not significantly improve log(E') prediction.

For tan δ prediction, the three VE256-based models had very similar performance. VE256WDNN3 has a marginal advantage in both test MSE loss and MAPE on tan δ peak over the other two models. We found that percolation, shifting factor, and broadening factor are highly correlated with either shelf error or peak error during our preliminary experiments. Thus, the result agrees with our preliminary experiments, showing that for tan δ prediction, it is worthwhile to pass the three features as wide signals directly to the last hidden layer. On the other hand, by comparing VE256 and VE256WDNN5, we can tell that wide signals must be carefully selected. Otherwise, including excessive features like particle radius mean and standard deviation may introduce noise and hurt the model performance.

Usually, it is meaningless to compare MSE loss of models predicting different targets as it is not normalized. Targets with values of order magnitude 10 will have 100 times bigger MSE loss than targets with values of order magnitude 1. In our case, however, since both log(E') data and tan δ data of the input VE master curves were scaled to 0 to 1, and the FEA simulated PNC VE master curves will not significantly deviate from this range, we can assume log(E') and tan δ curves of the PNC have similar range of value. Thus, we can roughly compare the test MSE loss between log(E') models and tan δ models. From Table 5, tan δ models tend to have higher test MSE loss than their log(E') twin, which is aligned with the fact that log(E') curves are simpler in shape compared to tan δ curves.

To provide a more rich comparison, we picked the best performing models for log(E') and tan δ prediction from Table 5, and visualized them on a random subset of test PS composite samples in Fig. 5.

Fig. 5 broadly agrees with the results of Table 5. The low MSE loss of both log(E') and tan δ in Table 5 translates into largely superposed curves for prediction and ground truth, though a few peak errors and shelf errors mentioned in Fig. 4 can be observed for tan δ.

3.2. Generalization from thermoplastics to thermosets

In this section, we take another step to test ViscoNet's generalization ability by evaluating predictions VE response curves for thermoset-based PNCs. The ViscoNet was pre-trained with 41,209 PC, 41,389 PMMA, and 34,964 PS data points, and then finetuned with 500 epoxy data points with an 80/20 train/valid split. Since there are about 50 % more data, the time consumption during the pre-training stage also increased by 50 %, resulting in around 45 min for tan δ models and 90 min for log(E') models. The finetuned model was then evaluated on an extra 22,505 epoxy data points. Once again, all epoxy data were simulated in FEA with newly generated microstructures. Table 6 summarizes the performance.

Overall, this thermoset finetuning case is comparable to the prior example of predictions for an unseen thermoplastic case. Increasing hidden dimension from 128 to 256 helps the performance while WDNN architecture has mixed but marginal impact on log

Table 5
Performance of ViscoNet models for generalization within thermoplastics.

Model	VE response	Test MSE loss	MAPE rubbery log modulus	MAPE glassy log modulus	MAPE tan δ peak
VE128np	E'	0.000180	5.85 %	0.41 %	
VE128	E'	0.000155	5.49 %	0.45 %	
VE256	E'	0.000137	4.90 %	0.34 %	
VE256WDNN5	E'	0.000144	5.93 %	0.35 %	
VE256WDNN3	E'	0.000144	5.04 %	0.38 %	
VE128np	tan δ	0.000912			5.03 %
VE128	tan δ	0.000835			4.83 %
VE256	tan δ	0.000740			4.51 %
VE256WDNN5	tan δ	0.000746			4.50 %
VE256WDNN3	tan δ	0.000720			4.45 %

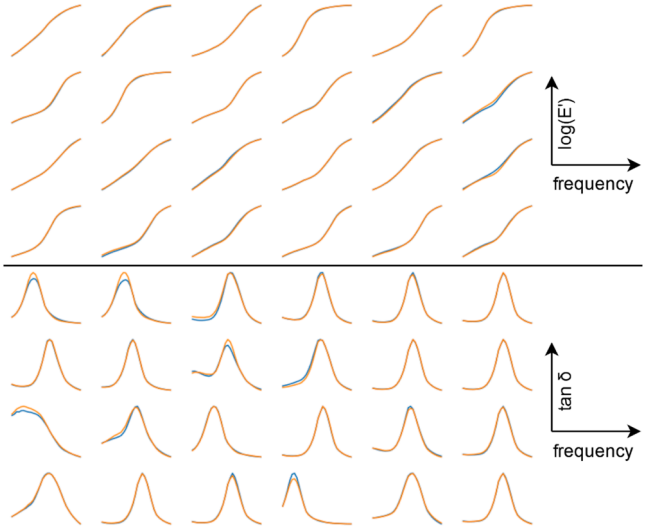

Fig. 5. Comparison between FEA simulated/ground truth (blue) and ViscoNet predicted (orange) log(E') curve by VE256 (top) and tan δ curve by VE256WDNN3 (bottom) after finetuning with 500 PS data.

(E') prediction. Compared to the previous case, it seems that ViscoNet did a slightly better job predicting rubbery modulus and a slightly poorer job predicting the glassy modulus for epoxy PNCs.

Interestingly, ViscoNet achieved much better results on tan δ prediction with test MSE loss lower than their log(E') twin and a tan δ peak MAPE lower than 2 %, despite the thermoplastic-to-thermoset generalization task should be more difficult due to the presence of a low-frequency plateau in log(E'). The additional 35k PS data for pretraining is a likely reason. By comparing VE128 and VE128np, the addition of the percolation signal significantly improves the tan δ prediction. We will discuss the impact of the percolation feature in detail in the next section. The selection of the best models for log(E') and tan δ prediction remains unchanged. Fig. 6 shows the ViscoNet vs. FEA visualizations randomly sampled from the epoxy test dataset.

3.3. Impact analysis on the percolation feature

From our experience of studying PNC viscoelastic responses, we hypothesize that the "shelf" error of tan δ prediction is highly correlated with interphase percolation. In this section, we seek to confirm or reject this hypothesis. VE128np and VE128 pre-trained with thermoplastics and finetuned with thermoset epoxy will be compared here. As we discussed earlier, the "shelf" error can be represented by a high MSE loss. Our first task is to determine a threshold for the MSE loss to be considered "high" in our case. Fig. 7 shows MSE loss progression in decile of the VE128np model.

We can tell that there is a sharp increase in MSE loss after the 90th percentile. The corresponding MSE loss is 0.0014, which we select as the threshold for determining high "shelf" error. With this threshold, we can compare the number of samples with/without high "shelf" error and their ratio for both VE128np and VE128 model and whether the sample is percolated or not. If percolation indeed has a big impact on "shelf" error, we expect to see significant with/without ratio change in percolated samples and a relatively stable with/without ratio in the rest samples listed in Table 7.

The numbers support our hypothesis. If we just look at the 13,854 percolated samples, VE128np, the model without the percolation feature, predicts 1 with high "shelf" error every 7 without. After the addition of the percolation feature in VE128, the ratio drops dramatically to 1 with high "shelf" error every 103 without, meaning the inclusion of the percolation feature significantly reduces

Table 6
Performance of ViscoNet models for generalization from thermoplastics to thermosets.

Model	VE response	Test MSE loss	MAPE rubbery modulus	MAPE glassy modulus	MAPE tan δ peak
VE128np	E'	0.000303	5.12 %	0.81 %	
VE128	E'	0.000303	5.00 %	0.89 %	
VE256	E'	0.000273	4.18 %	0.70 %	
VE256WDNN5	E'	0.000267	4.26 %	0.72 %	
VE256WDNN3	E'	0.000268	4.10 %	0.73 %	
VE128np	Tan δ	0.000645			2.68 %
VE128	Tan δ	0.000279			1.69 %
VE256	Tan δ	0.000189			1.37 %
VE256WDNN5	Tan δ	0.000201			1.27 %
VE256WDNN3	Tan δ	0.000191			1.22 %

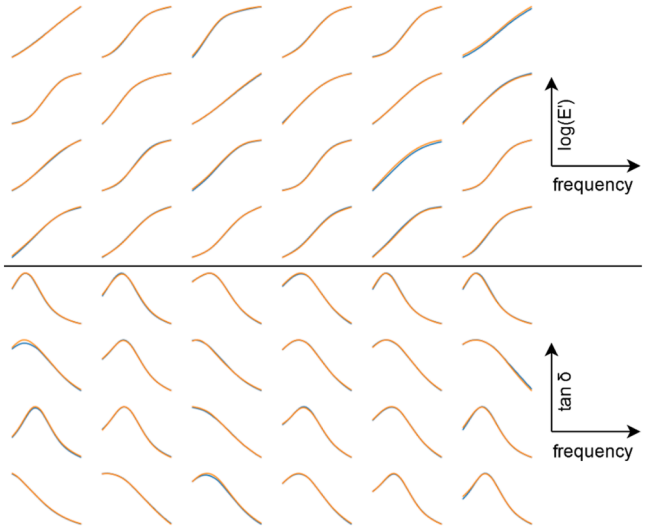

Fig. 6. Comparison between FEA simulated (blue) and ViscoNet predicted (orange) log(E') curve by VE256 (top) and tan δ curve by VE256WDNN3 (bottom) after finetuning with 500 epoxy data.

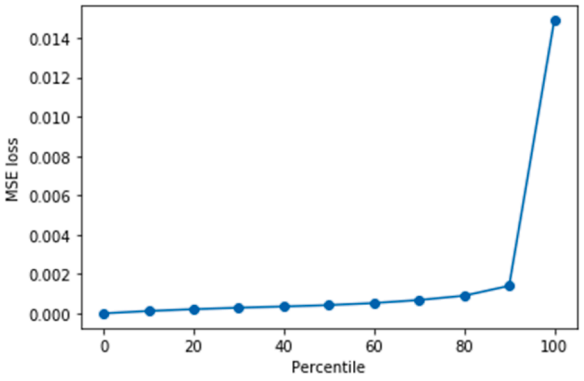

Fig. 7. The MSE loss progression of VE128np tan δ model (epoxy).

"shelf" error for percolated samples. As for the 8651 samples that are not percolated, the ratio slightly decreases from 0.063 to 0.046, which indicates the overall baseline improvement brought by the percolation feature. We can conclude that percolation is highly correlated with the "shelf" error in tan δ prediction. With that in mind, our next step is to evaluate the impact of the size of finetuning data on eliminating "shelf" and peak error.

3.4. Few-shot experiment for finetuning

For the pre-training-then-finetuning training scheme, an interesting question to ask is how much finetuning data will be enough. To answer this question, a few-shot experiment was conducted on the thermoplastics-to-thermoset tan δ prediction task with the best VE256WDNN3 ViscoNet model. Fig. 8 plots the test MSE loss and MAPE of tan δ peak with increasing finetuning epoxy data size.

Note that we apply 80/20 train/validation split to all finetuning data. The finetuning data size reflects the sum of train and valid

Table 7
Comparison of number of samples with/without "shelf" error before (VE128np) and after (VE128) the addition of percolation feature.

	without shelf error	with shelf error	ratio (with/without)
VE128np			
Percolated	12,113	1741	0.143
Not percolated	8141	510	0.063
VE128			
Percolated	13,721	133	0.010
Not percolated	8271	380	0.046

split. Test MSE loss converges at around 500 epoxy data and MAPE of tan δ peak is still slowly decreasing from 500 to 1000 epoxy data. Recall that we observed that "shelf" error is associated with the full-curve MSE loss, and the peak over- and under-prediction is associated with MAPE tan δ peak loss from our preliminary experiments with 10k PS data. The few-shot experiment suggests that finetuning with 500 epoxy data is sufficient for minimal "shelf" error and improved peak prediction, while further increasing the finetuning data size might further improve peak prediction. Fig. 9 visualizes the prediction history of a tan δ curve with an increasing finetuning epoxy data size.

Fig. 9 shows that the pre-trained model with 0 finetuning data can get the general shape of the tan δ curve correctly, demonstrating that it achieves a low order approximation of the VE response curve, but still the prediction is noticeably flawed with an MSE loss of 0.031, which is >160 times higher than the 0.000191 test MSE loss of the VE256WDNN3 model finetuned with 500 epoxy data as shown in Table 6. With more finetuning data, the "shelf" area converges to the ground truth quickly with around 200 samples. The closer the frequency is to the tan δ peak frequency, the slower the prediction of scaled tan δ converges to the ground truth. This observation is consistent with our interpretation of Fig. 8. Our conclusion is that 500 samples are sufficient for finetuning a good model. While more data can still improve the accuracy, the gains in accuracy are marginal after a few hundred fine tuning samples.

3.5. Time consumption analysis

In this section, we provide an estimation on how much time can be saved by using ViscoNet as a surrogate model for FEA simulation of VE response. Since the pretrained model is readily available online, we will not include the time consumption for pretraining in this calculation. According to the few-shot experiment, researchers can run as few as 500 FEA simulations for the model to predict reasonably well on a new thermoplastic/thermoset silica nanocomposite system. In prior works, researchers note that the magnitude of NP modulus and isotropy have minimal impact on the PNC VE response (Qiao and Catherine Brinson, 2009), and thus the number of additional data and time for finetuning for a PNC with a new NP is expected to be low. In our FEA settings, it takes about 7 min for a 500-by-500 RVE simulation using 4 CPU cores. Thus, 500 simulations take ~58.3 h. With these 500 VE response data, the pretrained ViscoNet model (VE256 for log(E') and VE256WDNN3 for tan δ) can be finetuned (without GPU) for 50 epochs on 1 CPU within 15 min with parallel data loading turned off, mimicking a low-resource setup.

From that point on, ViscoNet can be used to generate a surrogate VE response that is within 5 % MAPE for rubbery modulus, 1 % MAPE for glassy modulus, and 2 % MAPE for tan δ peak when compared to the FEA simulated VE response resulting from those same inputs, based on Table 6. The inference time with ViscoNet is negligible compared to FEA simulation. ViscoNet can generate 20k+ VE response within 2 min using a batch size of 1 and parallel data loading disabled, which otherwise takes FEA 140k minutes on 4 CPU cores, or 117 h on 80 CPU cores assuming the simulation speed grows linearly with the number of cores. If we lift the resource limit on ViscoNet, with a batch size of 10k and 10 workers for data loading, ViscoNet can generate 1.3 million VE responses within 38 s.

Putting this all together, ViscoNet is a powerful yet lightweight surrogate model for FEA simulation of VE response of PNCs. Unlike many other surrogate models that generate a single scalar property value at a specific frequency, like tan δ peak or glassy modulus (Wang et al., 2020), ViscoNet generates the full VE response curve itself with a transformation that flattens the curve into a sequence of VE response by fixing a finite number of frequencies of interest. Since the scalar properties are derived from the full curve, ViscoNet exceeds the capabilities of prior models. Simultaneously, ViscoNet is low-resource friendly due to the relatively small number of parameters needed. No GPU is required for finetuning or inference, and data parallelism was not enabled for the time consumption estimations above.

Because of these capabilities, researchers can use ViscoNet to quickly populate a database within minutes using only 500 seed FEA simulations to finetune ViscoNet. Metamodeling and optimization can then be done with the populated database (Marr et al., 2023). Furthermore, ViscoNet lowers the entrance bar to the data science part of the PNC design world and promotes the accessibility of data-driven 2D materials design of PNCs by enabling anyone with Internet access to finetune a model on their laptop. If computation of 500 initial FEA simulations remains a barrier, archived FEA simulations may be found in data archive resources such as MaterialsMine.

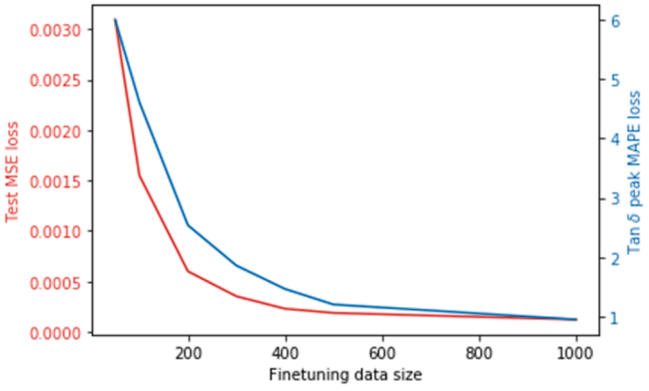

Fig. 8. Few-shot analysis of MSE loss and tan δ peak MAPE loss on epoxy test dataset using VE256WDNN3 model finetuned with increasing number of epoxy data.

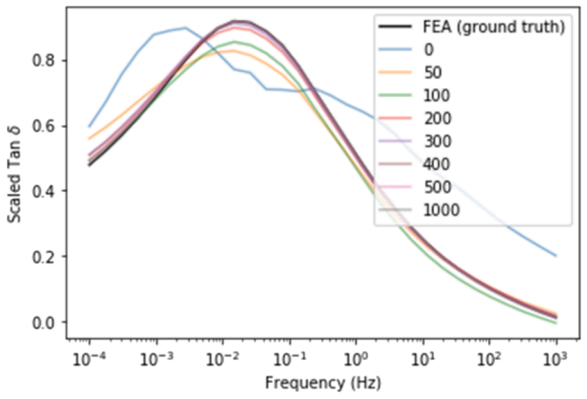

Fig. 9. Prediction history of an epoxy tan δ curve with increasing finetuning data size.

3.6. Use case scenarios

In this section, we demonstrate how ViscoNet can be applied to quantify the role of interphase in PNC VE response with a case study. A specific microstructure of epoxy-nanosilica is selected for the study, as shown in Fig. 10, with particle radius 40 ± 20 nm, filler volume fraction 0.15, and shifting and broadening factors fixed at -2. The microstructure is generated fresh for the case study, so it is unseen data for ViscoNet.

The ViscoNet-generated tan δ curve and the peak height/frequency are tracked with an interphase thickness varying from 0 to 50 pixels, corresponding to 0 to 100 nm. The 50 ViscoNet inferences, with an interphase growth of 1 pixel at each step, take <1 second in total. To validate the result, 10 full FEA simulations are independently run with an interphase growth of 5 pixels at each step, which takes >1 hour in total, massively slower than ViscoNet. Fig. 11 shows the response of full tan δ curve from each interphase fraction with a side-by-side comparison of FEA simulated results and ViscoNet generated results.

ViscoNet successfully reproduces the FEA simulations on this new microstructure, but with a finer granularity, helping to reveal the impact of percolation on the tan δ response. In the ViscoNet tan δ response plot, a clear gap between the responses can be observed when percolation starts (dark orange curve), which cannot be easily found in the FEA plot due to the low granularity caused by the time and resource restrictions. The tan δ curve of pure epoxy (solid black curve) and interphase after shifting and broadening (dashed black curve) are also provided as a reference. With low interphase fraction (Vt), tan δ curve is dominated by bulk epoxy. With increasing Vt, the tan δ curve starts to be dominated by the interphase. The gap as we mentioned earlier indicates that percolation boosts the transition of a bulk-epoxy-dominant tan δ curve into an interphase-dominant tan δ curve. Note that all FEA simulated and ViscoNet predicted tan δ curves never leave the region bounded by the two reference curves of bulk epoxy and interphase, creating visual "stationary points" in the data series where these curves cross.

Looking at tan δ peak height and frequency as a function of Vt in Fig. 12 reveals that peak height decreases initially with Vt and then increases, while peak frequency gradually decreases by 2 decades. Fig. 12 also includes the response of tan δ peak height and frequency to Vt with varying broadening factors. Three major impacts on the response of tan δ peak height to Vt can be observed from increasing the broadening factor from 1, meaning no broadening (dashed line), to 2 (solid line) and 3 (dotted line).

1. A larger broadening factor tends to weaken the impact of Vt on tan δ peak height – The stationary point at which the flatter interphase curve intersects with the bulk epoxy curve at a higher tan δ, causes the lower bound of the tan δ peak height with varying Vt to increase, leaving less room for tan δ peak height to change as illustrated in Fig. 13.
2. Increasing the broadening factor extends the zone of decreasing tan δ peak height past the percolation point – With no broadening, the peak height of the compsite at percolation (Vt = 0.39) coincides with the low frequency stationary point of that case, and this is the minimum peak height. Broadening factors of 2 and 3 shift the peak height at percolation to the right and also delay the increase until 0.5–0.6 and 0.6–0.7, respectively.
3. The broadening factor causes and increase in the tan δ peak height at percolation – At percolation, there is likely a "bridged" effect described by Senses, et al. (Senses et al., 2017), where a network is formed with bridged polymer chains and nanoparticles, resulting in a significant change in the viscoelastic behavior of PNCs. Large broadening factors and the "bridged" effect amplify each other, leading a bump in tan δ peak height.

Considering the discussion above about the impact of broadening and Vt on the viscoelastic behavior of PNCs, the parameter we have best control over in the lab is Vt via designed chemistries and surface interactions. To better understand the physical implication of the observations, it is worthwhile to interpret with some intuition about tan δ and interphase fraction Vt. The tan δ indicates the ratio of dissipated energy to the stored energy of the material system when a load is applied. For a viscoelastic material, a high tan δ peak suggests that the material is more to the viscous end, and a low tan δ peak suggests it to be more elastic. The case study shows that the tan δ peak height is usually not linearly correlated with the filler fraction as nanoparticles can aggregate. Vt is directly impacted by the

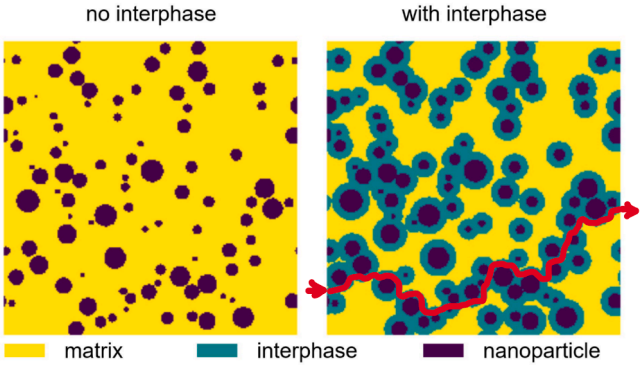

Fig. 10. Microstructure of the epoxy-nanosilica composite (left) and its microstructure with a percolated interphase with a thickness of 13 pixels/26 nm (right) for the use case demo. The percolation pathway is in red.

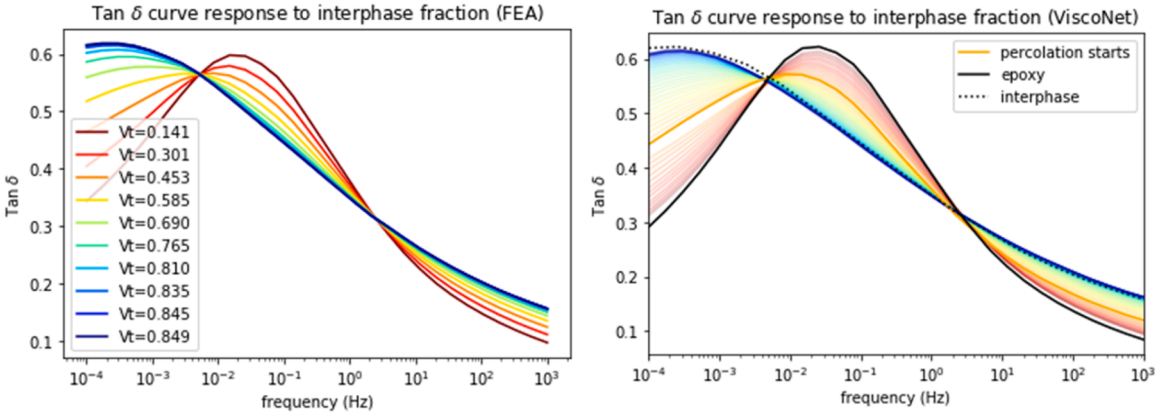

Fig. 11. Tan δ curve response to interphase fraction, left: FEA, right: ViscoNet. Vt stands for the volume fraction of the interphase; broadening factor = 2 for this case. Stationary points occur where the interphase and matrix curves intersect. See supporting information for additional broadening factor values.

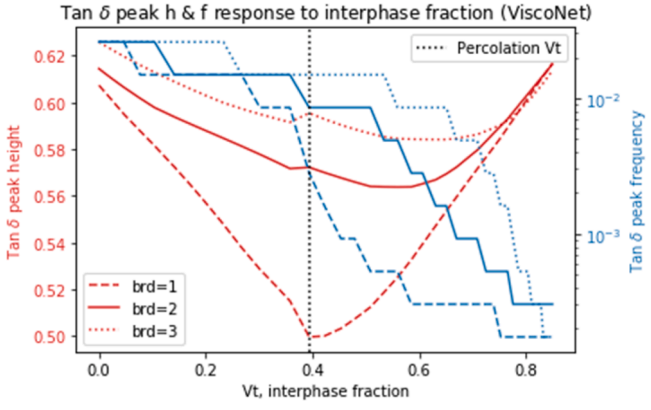

Fig. 12. ViscoNet-generated tan δ peak height and frequency as a function of interphase fraction Vt with a shifting factor of −2 and a broadening factor of 1 (dashed), 2 (solid), and 3 (dotted).

dispersion of nanoparticles and the thickness of the interphase, which can be interpreted as the region where the mobility of polymer chains is impacted by the confinement introduced by the addition of nanoparticles. Thus, surface modification can significantly increase Vt as it not only brings potentially better dispersion, but also impacts more polymer chains in bulk polymer matrix with the grafted chains via entanglement. Besides surface modification, there are other approaches to control Vt. Huang et al. conducted a

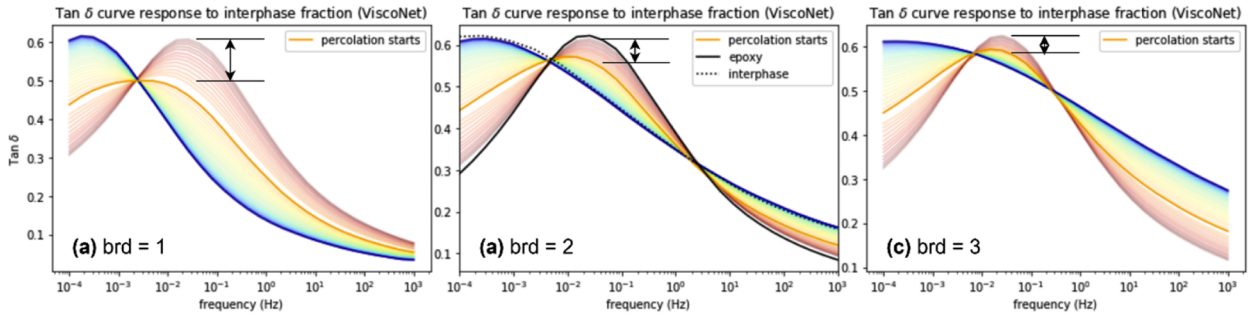

Fig. 13. Tan δ curve response to interphase fraction with a broadening factor of (a) 1, (b) 2, and (c) 3. The range of tan δ peak height is illustrated with bars and arrows in each diagram.

comprehensive survey summarizing the current knowledge of interphase and practical experience on controlling the interphase (Huang et al., 2022). It is concluded in their work that the interphase thickness is directly impacted by the radius of gyration (Rg) and molecular structure of the polymer chain adsorbed to the surface of nanoparticles. Therefore, increasing the molecular weight of polymer matrix should lead to a bigger Rg, a thicker interphase, and hence a larger Vt. In fact, Huang et al. summarized that there is a propagated impact via the entangled polymer chains that impacts the chain relaxation behavior in a range of 3–11 Rg from the interface (Huang et al., 2022). Thus, finding ways to increase chain entanglement could result in a high Vt by leveraging the propagated impact.

This case study demonstrates that the fast inference speed of ViscoNet and its lightweight nature enables researchers to generate a large amount of data with fine granularity. The fine granularity helps reveal the impact of percolation on tan δ curve, which is otherwise easily overlooked by FEA simulations due to its prohibitively high computational cost of fine-grained exploration.

3.7. Limitations

There are still a small number of extreme cases (< 3 %) in which ViscoNet provides poor predictions, with MSE error > 0.002. We believe this limitation can be overcome with more pretraining data. Over time, more FEA data will be generated and curated into MaterialsMine, enabling better pretraining, benchmarking, and analysis. Another limitation is that the current version of ViscoNet trained on PNCs with silica NPs as the filler, 2D microstructure geometries with no agglomerations, and a relatively narrow frequency ranging from 10^{-4} Hz and 10^{3} Hz. This limitation will be addressed in future work by expanding the training to alternate microstructures, such as beyond spheroidal nanofillers. The current 2D capability of ViscoNet is a limitation for real PNC design, which requires 3D simulation. Currently, ViscoNet represents the initial step toward making PNC design accessible at the 2D level. One of our ongoing efforts is to develop a surrogate model that predicts 3D responses based on 2D slices, which aims to bridge this gap. This work used a uniform interphase representation for FEA simulation due to simplicity concern. In the future, a gradient interphase representation with better compliance with experimental data could be adopted (Li et al., 2019), since the existence of a gradient in the interphase was reported by multiple authors (Huang et al., 2022), (Xu et al., 2017). Finally, we suggest that in general using Prony series instead of the frequency sweep to represent the VE response could introduce better generalization ability to ViscoNet (Park and Schapery, 1999), (Bradshaw and Brinson, 1999).

4. Conclusion

In this work, we propose ViscoNet, a novel surrogate model for finite element analysis (FEA) simulations of PNC viscoelastic (VE) response. The 2D VE response curves are reduced to feature vectors by fixing the frequencies of interest. To make ViscoNet compatible for any PNC, VE response curves (log(E') and tan δ) are scaled by the max and min value of those of the pure polymer matrices. We explored different model architectures with varying hidden sizes and a WDNN design, with and without the percolation flag. Compared to log(E'), predicting tan δ curve is relatively difficult due to its non-monotonic shape, leading to a "shelf" error, captured by the full-curve MSE loss, or a peak error, captured by the MAPE loss of tan δ peak.

Two experiments were conducted to evaluate the generalization ability of ViscoNet. First, for log(E') prediction of PC/PMMA PNC data and finetuned with PS PNC data using unseen microstructures, ViscoNet models excelled in predicting glassy modulus with an MAPE around 0.3 %−0.4 % and performed well in predicting rubbery modulus with an MAPE around 4 %−5 %. VE256, a deep NN model with 2 hidden layers of size 256 dimensions, achieved the best performance in predicting log(E'), with the addition of wide signals showing marginal impact, suggesting simpler E' curves benefit less from complex structures like WDNN. For tan δ prediction, a model which includes percolation, shifting factor, and broadening factor as wide signals, showcased a slight advantage in test MSE (0.00072) and MAPE on the peak (4.45 %). The importance of careful selection of wide signals is evident, with excessive features potentially introducing noise.

The second experiment pre-trained ViscoNet with thermoplastic PC/PMMA/PS PNC data, and then finetuned with epoxy PNC data, again using unseen microstructures. The findings parallel those of the thermoplastic-to-unseen thermoplastic scenario. Increasing the

hidden dimension from 128 to 256 enhances performance, while WDNN moderately impacts log(E') prediction. Compared to the first experiment, ViscoNet slightly improved rubbery modulus prediction towards the lower end of the 4 %−5 % MAPE loss, but was slightly less accurate in predicting glassy modulus for epoxy PNCs with an MAPE of 0.7 %−0.8 %. ViscoNet showed notable success in this case for tan δ prediction, with lower test MSE loss and tan δ peak MAPE below 2 %, likely due to additional pre-training with 35k PS data.

The percolation feature significantly reduces the ratio of samples with "shelf" error vs. samples without "shelf" error from 0.143 to 0.010 on the epoxy dataset. The few-shot experiment suggests that finetuning with 500 epoxy data is sufficient for minimal "shelf" error and acceptable peak prediction, while further increasing the finetuning data size to 1000 only marginally improves peak prediction.

ViscoNet can generate 20k+ VE response within 2 min using a batch size of 1 and parallel data loading disabled with 1 CPU core, which would otherwise take FEA 140k minutes on 4 CPU cores, or 117 h on 80 CPU cores assuming the simulation speed grows linearly with the number of cores. This fast, low-resource, yet reliable approach significantly enhances the accessibility of data-driven materials design of PNCs. In a VE material design loop, ViscoNet enables insights and discoveries by either replacing the FEA simulation component as a surrogate or by directly filling the design space, thanks to its exceptionally rapid inference speed.

CRediT authorship contribution statement

Anqi Lin: Writing – review & editing, Writing – original draft, Visualization, Validation, Supervision, Software, Methodology, Investigation, Formal analysis, Data curation, Conceptualization. **Richard J. Sheridan:** Writing – review & editing, Supervision, Software, Project administration, Conceptualization. **Bingyin Hu:** Writing – review & editing, Software, Conceptualization. **L. Catherine Brinson:** Writing – review & editing, Resources, Funding acquisition, Supervision, Conceptualization.

Declaration of competing interest

The authors declare that they have no known competing financial interests or personal relationships that could have appeared to influence the work reported in this paper.

Acknowledgements

The authors would like to acknowledge Tolulomo Fateye, Dr. Marc Palmeri, and Dr. Jamie McCusker for their efforts in building the MaterialsMine data ingestion pathway for FEA data.

Supplementary materials

Supplementary material associated with this article can be found, in the online version, at doi:10.1016/j.jmps.2024.105915.

Data availability

The PyTorch script and the pre-trained model artifact are available at https://github.com/anqiclaire/VE-FEA-surrogate. The FEA simulation data used for model training is available from the Duke Research Data Repository at https://doi.org/10.7924/r4g166t5p. Existing and additional FEA data is being curated into MaterialsMine (https://materialsmine.org) to enable better pretraining, benchmarking, and analysis.

References

Alves, N.M., Gómez Ribelles, J.L., Gómez Tejedor, J.A., Mano, J.F., 2004. Viscoelastic behavior of poly(methyl methacrylate) networks with different cross-linking degrees. Macromolecules 37 (10), 3735–3744. https://doi.org/10.1021/ma035626z.

Bradshaw, R.D., Brinson, L.C., 1999. Mechanical response of linear viscoelastic composite laminates incorporating non-isothermal physical aging effects. Compos. Sci. Technol. 59 (9), 1411–1427. https://doi.org/10.1016/S0266-3538(98)00179-1.

Brinson, L.C., et al., 2020. Polymer nanocomposite data: curation, frameworks, access, and potential for discovery and design. ACS Macro Lett. 9 (8), 1086–1094. https://doi.org/10.1021/ACSMACROLETT.0C00264/ASSET/IMAGES/LARGE/MZ0C00264_0006.JPEG.

Cavaille, J.Y., Jourdan, C., Perez, J., Monnerie, L., Johari, G.P., 1987. Time-temperature superposition and dynamic mechanical behavior of atactic polystyrene. J. Polym. Sci. Part B Polym. Phys. 25 (6), 1235–1251. https://doi.org/10.1002/polb.1987.090250605.

Chen, W., et al., 2020a. Materials informatics and data system for polymer nanocomposites analysis and design," in *Handbook on Big Data and Machine Learning in the Physical Sciences*, 2 vols. World Scientific Series On Emerging Technologies. World Scientific, pp. 65–125. https://doi.org/10.1142/9789811204555_0003.

Chen, Q., Tu, W., Ma, M., 2020b. Deep learning in heterogeneous materials: targeting the thermo-mechanical response of unidirectional composites. J. Appl. Phys. 127 (17).

Chen, Q., Jia, R., Pang, S., 2021. Deep long short-term memory neural network for accelerated elastoplastic analysis of heterogeneous materials: an integrated data-driven surrogate approach. Compos. Struct. 264, 113688.

Cheng, H.-T., et al., 2016. Wide & deep learning for recommender systems. arXiv. https://doi.org/10.48550/arXiv.1606.07792.

Deagen, M.E., Brinson, L.C., Vaia, R.A., Schadler, L.S., 2022. The materials tetrahedron has a 'digital twin. MRS Bull. 47 (4), 379–388. https://doi.org/10.1557/S43577-021-00214-0/TABLES/2.

Devlin, J., Chang, M.-W., Lee, K., Toutanova, K., 2019. BERT: pre-training of Deep Bidirectional Transformers for Language Understanding. arXiv. https://doi.org/10.48550/arXiv.1810.04805.

Faupel, F., Zaporojtchenko, V., Strunskus, T., Elbahri, M., 2010. Metal-polymer nanocomposites for functional applications. Adv. Eng. Mater. 12 (12), 1177–1190. https://doi.org/10.1002/adem.201000231.
Fisher, F.T., Eitan, A., Andrews, R., Schadler, L.S., Brinson, L.C., 2004. Spectral response and effective viscoelastic properties of Mwnt-reinforced polycarbonate. Adv. Compos. Lett. 13 (2), 096369350401300201. https://doi.org/10.1177/096369350401300201.
Gossett, E., et al., 2018. AFLOW-ML: a RESTful API for machine-learning predictions of materials properties. Comput. Mater. Sci. 152 (November 2017), 134–145. https://doi.org/10.1016/j.commatsci.2018.03.075.
Hashemi, A., Jang, J., Beheshti, J., 2023. A machine learning-based surrogate finite element model for estimating dynamic response of mechanical systems. IEEE Access 11, 54509–54525. https://doi.org/10.1109/ACCESS.2023.3282453.
Hendrycks, D., Gimpel, K., 2023. Gaussian error linear units (GELUs). arXiv. https://doi.org/10.48550/arXiv.1606.08415.
Himanen, L., Geurts, A., Foster, A.S., Rinke, P., 2019. Data-driven materials science: status, challenges, and perspectives. Adv. Sci. 6 (21). https://doi.org/10.1002/advs.201900808.
Hochreiter, S., Schmidhuber, J., 1997. Long short-term memory. Neur. Comput. 9 (8), 1735–1780.
Huang, J., Zhou, J., Liu, M., 2022. Interphase in polymer nanocomposites. JACS Au 2 (2), 280–291. https://doi.org/10.1021/jacsau.1c00430.
Khan, M., et al., 2015. Graphene based metal and metal oxide nanocomposites: synthesis, properties and their applications. J. Mater. Chem. A 3 (37), 18753–18808. https://doi.org/10.1039/C5TA02240A.
LeCun, Y., Bottou, L., Bengio, Y., Haffner, P., 1998. Gradient-based learning applied to document recognition. Proc. IEEE 86 (11), 2278–2324.
Li, Y., Zhao, B., Xie, S., Zhang, S., 2003. Synthesis and properties of poly(methyl methacrylate)/montmorillonite (PMMA/MMT) nanocomposites. Polym. Int. 52 (6), 892–898. https://doi.org/10.1002/pi.1121.
Li, X., et al., 2019. Rethinking interphase representations for modeling viscoelastic properties for polymer nanocomposites. Materialia 6, 100277. https://doi.org/10.1016/j.mtla.2019.100277.
Liu, Z., Moore, J.A., Liu, W.K., 2016. An extended micromechanics method for probing interphase properties in polymer nanocomposites. J. Mech. Phys. Solids 95, 663–680. https://doi.org/10.1016/j.jmps.2016.05.002.
Liu, X., Tian, S., Tao, F., Yu, W., 2021. A review of artificial neural networks in the constitutive modeling of composite materials. Compos. Part B Eng. 224, 109152. https://doi.org/10.1016/j.compositesb.2021.109152.
Marr, J., Zartmann, L., Reinel-Bitzer, D., Andrä, H., Müller, R., 2023. Multiscale optimization of the viscoelastic behavior of short fiber reinforced composites. Int. J. Mech. Mater. Des. 19 (3), 501–519. https://doi.org/10.1007/s10999-023-09645-w.
Mehl, M.J., et al., 2017. The AFLOW library of crystallographic prototypes: part 1. Comput. Mater. Sci. 136, S1–S828. https://doi.org/10.1016/j.commatsci.2017.01.017.
Nie, Z., Jiang, H., Kara, L.B., 2020. Stress field prediction in cantilevered structures using convolutional neural networks. J. Comput. Inf. Sci. Eng. 20 (1), 011002.
OpenAI, 2023. GPT-4 Technical Report. arXiv. https://doi.org/10.48550/arXiv.2303.08774.
Park, S.W., Schapery, R.A., 1999. Methods of interconversion between linear viscoelastic material functions. Part I—a numerical method based on Prony series. Int. J. Solid. Struct. 36 (11), 1653–1675. https://doi.org/10.1016/S0020-7683(98)00055-9.
Pham, V.H., Dang, T.T., Hur, S.H., Kim, E.J., Chung, J.S., 2012. Highly conductive poly(methyl methacrylate) (PMMA)-reduced graphene oxide composite prepared by self-assembly of PMMA latex and graphene oxide through electrostatic interaction. ACS Appl. Mater. Interfaces 4 (5), 2630–2636. https://doi.org/10.1021/am300297j.
Prabhune, P., et al., 2023. Design of polymer nanodielectrics for capacitive energy storage. Nanomaterials 13 (17). https://doi.org/10.3390/nano13172394. Art. no. 17.
Qiao, R., Catherine Brinson, L., 2009. Simulation of interphase percolation and gradients in polymer nanocomposites. Compos. Sci. Technol. 69 (3), 491–499. https://doi.org/10.1016/j.compscitech.2008.11.022.
Raffel, C., et al., 2020. Exploring the Limits of Transfer Learning with a Unified Text-to-Text Transformer. arXiv. https://doi.org/10.48550/arXiv.1910.10683.
Rumelhart, D.E., Smolensky, P., McClelland, J.L., Hinton, G., 1986. Sequential thought processes in PDP models. Parall. Distrib. Process. Explor. Microstruct. Cogn. 2, 3–57.
Schadler, L.S., et al., 2020. A perspective on the data-driven design of polymer nanodielectrics. J. Phys. Appl. Phys. 53 (33), 333001. https://doi.org/10.1088/1361-6463/ab8b01.
Senses, E., Narayanan, S., Mao, Y., Faraone, A., 2017. Nanoscale particle motion in attractive polymer nanocomposites. Phys. Rev. Lett. 119 (23), 237801. https://doi.org/10.1103/PhysRevLett.119.237801.
Song, Y., Zheng, Q., 2015. Linear rheology of nanofilled polymers. J. Rheol. 59 (1), 155–191. https://doi.org/10.1122/1.4903312.
Wang, M., Pramoda, K.P., Goh, S.H., 2005. Enhancement of the mechanical properties of poly(styrene-co-acrylonitrile) with poly(methyl methacrylate)-grafted multiwalled carbon nanotubes. Polym. (Guildf) 46 (25), 11510–11516. https://doi.org/10.1016/j.polymer.2005.10.007.
Wang, Y., et al., 2018. Identifying interphase properties in polymer nanocomposites using adaptive optimization. Compos. Sci. Technol. 162, 146–155. https://doi.org/10.1016/j.compscitech.2018.04.017.
Wang, Y., et al., 2020. Mining structure–property relationships in polymer nanocomposites using data driven finite element analysis and multi-task convolutional neural networks. Mol. Syst. Des. Eng. 5 (5), 962–975.
Woo, E.M., Seferis, J.C., Schaffnit, R.S., 1991. Viscoelastic characterization of high performance epoxy matrix composites. Polym. Compos. 12 (4), 273–280. https://doi.org/10.1002/pc.750120408.
Wu, L., Kilingar, N.G., Noels, L., 2020. A recurrent neural network-accelerated multi-scale model for elasto-plastic heterogeneous materials subjected to random cyclic and non-proportional loading paths. Comput. Method. Appl. Mech. Eng. 369, 113234.
Xu, J., et al., 2017. Mobility gradient of poly(ethylene terephthalate) chains near a substrate scaled by the thickness of the adsorbed layer. Macromolecules 50 (17), 6804–6812. https://doi.org/10.1021/acs.macromol.7b00922.
Xu, H., et al., 2021. Data-driven multiscale science for tire compounding: methods and future directions," in *Theory and Modeling of Polymer Nanocomposites*. In: Ginzburg, V.V., Hall, L.M. (Eds.), Springer Series in Materials Science. Springer International Publishing, Cham, pp. 281–312. https://doi.org/10.1007/978-3-030-60443-1_11.
Yao, H., Gao, Y., Liu, Y., 2020. FEA-Net: a physics-guided data-driven model for efficient mechanical response prediction. Comput. Method. Appl. Mech. Eng. 363, 112892.
Zare, Y., Rhee, K.Y., 2018. Evaluation and development of expanded equations based on Takayanagi model for tensile modulus of polymer nanocomposites assuming the formation of percolating networks. Phys. Mesomech. 21 (4), 351–357. https://doi.org/10.1134/S1029959918040094.
Zhang, Z., Friedrich, K., 2003. Artificial neural networks applied to polymer composites: a review. Compos. Sci. Technol. 63 (14), 2029–2044. https://doi.org/10.1016/S0266-3538(03)00106-4.
Zhang, Z., Klein, P., Friedrich, K., 2002. Dynamic mechanical properties of PTFE based short carbon fibre reinforced composites: experiment and artificial neural network prediction. Compos. Sci. Technol. 62 (7), 1001–1009. https://doi.org/10.1016/S0266-3538(02)00036-2.
Zhao, H., Li, X., Zhang, Y., Schadler, L.S., Chen, W., Brinson, L.C., 2016. Perspective: nanoMine: a material genome approach for polymer nanocomposites analysis and design. APL Mater. 4 (5), 053204. https://doi.org/10.1063/1.4943679.
Zhao, H., et al., 2018. NanoMine schema: an extensible data representation for polymer nanocomposites. APL Mater. 6 (11), 111108. https://doi.org/10.1063/1.5046839.

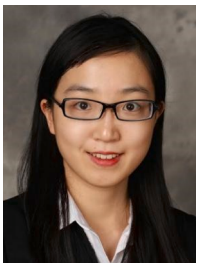

Anqi Lin received her B.Eng. degree in Aircraft Engineering at Tongji University, Shanghai, China. She received her M.S. degree in Materials Science and Engineering at Northwestern University, IL, USA. She is graduating with her Ph.D. in Mechanical Engineering and Materials Science at Duke University, NC, USA. Her research interests include data curation, machine learning, and data-driven material design.

Richard Sheridan is a Research Scientist in the Brinson Advanced Materials Laboratory at the Duke University Department of Mechanical Engineering and Materials Science. Richard received his Ph.D. from the University of Colorado at Boulder studying the rheology and applications of thermoreversible polymer networks. He then accepted a postdoc at the NIST where he researched the physics and metrology of polymer films and interfaces. Subsequently, he was a NIST-CHiMaD fellow measuring the interphase properties of fiberglass materials. His current research interests include optimal experimental design, uncertainty quantification, and AI-augmented laboratory techniques, especially in the context of AFM nanomechanics.

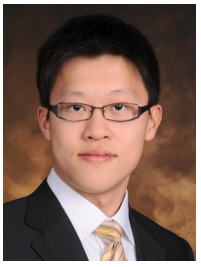

Bingyin Hu received his Ph.D. in Mechanical Engineering and Materials Science and M.S. in Electrical and Computer Engineering at Duke University, NC, USA. Prior to that, he received his B.Eng. degree in Environmental Engineering at Tsinghua University, Beijing, China and M. S. degree in Civil and Environmental Engineering at Carnegie Mellon University, PA, USA. His research interests include materials informatics, natural language processing, and data curation with a special focus on utilizing natural language processing to extract structured data from unstructured polymer nanocomposites publications.

Cate Brinson is the Sharon and Harold Yoh Professor and Donald Alstadt Department Chair of the Mechanical Engineering and Materials Science Department at Duke University. She obtained her phd from Caltech and was faculty at Northwestern University prior to Duke. Current work includes characterization, modeling and data science applied to polymers/composites/metamaterials. Her awards include the Eringen Medal of SES, the Nadai Medal of ASME, the Bessel Prize of the Humboldt Foundation and she is a Fellow of many professional societies. She served on the SES Board of Directors and is a founding member of the Materials Research Data Alliance (MaRDA).